Direct Measurement of the Applied-Field Component of the Thrust of a Lithium Lorentz Force Accelerator

William J. Coogan,* Michael A. Hepler,* and Edgar Y. Choueiri†
Princeton University, Princeton, NJ, 08544, USA

The operation of an inverted-pendulum thrust stand designed to directly measure the applied-field thrust component of a steady-state applied-field magnetoplasmadynamic thruster is presented. This measurement, which is necessary for improving and validating thrust models, is achieved by mechanically isolating the solenoid from the thruster so that the solenoid can move independently. The deflection of the solenoid is compared to deflection by known forces to determine the applied-field thrust component. The thrust stand is found to be accurate to ±9 mN over a total range of 1200 mN. Two measurement methods are implemented to account for tare forces resulting from azimuthal currents to the thruster electrodes and are shown to agree with one another. As a proof-of-concept, the first direct measurements of the applied-field component of the thrust from a 30 kW lithium Lorentz force accelerator operating at 400 A, 8 mg/s lithium mass flow rate, and 0.056 T applied-field strength give a measured force of 108 ± 14 mN. This measurement agrees with the value predicted by measuring the total thrust and subtracting out all other thrust components.

Nomenclature

a_0	Ion sound speed, m/s
A	Area, m^2
B_A	Applied magnetic field, T
J	Current, A
k	Thrust coefficient
$\dot{m}$	Mass flow rate, kg/s
p	Pressure, N/m^2
r	Electrode radius, m
T	Thrust, N

Subscript

ae	Anode exit plane
AF	Applied-field
c	Cathode
GD	Gasdynamic
SF	Self-field

I. Introduction

The applied-field magnetoplasmadynamic thruster (AF-MPDT) is a high thrust-density electric propulsion device typically consisting of an annular anode surrounding a central cathode with a solenoid generating a magnetic field along the thrust axis. Many theoretical thrust models have been presented for the AF-MPDT,[1–7] and while there is a general consensus that the thrust is proportional to both the current

*Graduate Student, MAE Dept., Princeton University, AIAA Student Member.
†Chief Scientist, EPPDyL, Professor, Applied Physics Group, MAE Dept., Princeton University, AIAA Fellow.

through the electrodes and the strength of the applied magnetic field, a complete model in terms of controllable parameters, such as the propellant type, mass flow rate, electrode geometry, applied-field strength, and thruster current, has yet to be agreed upon.

There are three thrust generating mechanisms in an AF-MPDT, which we will call self-field (SF), gasdynamic (GD), and applied-field (AF) thrust components. For each thrust component, there is a power regime where that particular component is large compared to the other two. The SF thrust component, for example, is the primary thrust mechanism for SF-MPDTs, and results from the interaction of the current with its own self-induced magnetic field. The SF thrust component is dominant at high power in AF-MPDTs, typically in the mid-100s of kW to MW, well-beyond the steady-state capacity of existing space-based power supplies. The GD thrust component is the result of the conversion of thermal energy to directed kinetic energy by means of a nozzle. For our 30 kW lithium Lorentz Force Accelerator (LiLFA), a lithium-fed AF-MPDT, operating with typical parameters of 20 mg/s mass flow rate and 0.1 T AF strength, the GD thrust component is dominant up to around 15 kW. Both SF and GD thrust components have theoretical models validated by experimental results.[8,9]

For power levels from the 10s to mid-100s of kW, the AF thrust component is dominant. This power regime is of particular interest since power levels between 100-200 kW are anticipated in the near- to mid-term for space missions.[10] Existing theoretical models for the AF thrust component have previously been compared to values inferred from measurements of the total thrust. To determine the AF component, the theoretical values for the self-field and gasdynamic components were subtracted from the total, so that

$$T_{\mathrm{AF}} = T - T_{\mathrm{SF}} - T_{\mathrm{GD}}, \tag{1}$$

where T_{AF} is the applied-field thrust component, T is the total thrust, T_{SF} is the self-field thrust component, and T_{GD} is the gasdynamic thrust component.[2,5–7] While this theoretically provides the AF thrust component, the magnitude of the error on the final value is undeterminable without individual measurements of T_{SF} and T_{GD} along with the corresponding error on each component. Tahara et al. inferred values of each of the three components through the measurement of pressure, current, and magnetic field distributions within the thruster volume,[3] but this is still an indirect measurement of the force from each component with undeterminable error. In order to validate an AF thrust model, we seek a method of bounding the uncertainty in the value T_{AF} by measuring it directly.

With this purpose, we have constructed and tested a novel thrust stand with which to make an isolated measurement of T_{AF} since this is the thrust component primarily responsible for disagreement between thrust models. In Section II, we provide a description of two thrust models from the literature, each possessing a nondimensional free parameter of unknown dependencies, and which varies greatly from one thruster to another, motivating direct measurement of this thrust component. We describe our thrust stand and calibration procedure in Section III. In Section IV, we present the first direct measurements of the force generated by the AF component of the thrust of our 30 kW LiLFA.

II. Thrust Model Comparison

Of the existing thrust models in the literature, only two offer expressions for the AF component of the thrust in terms of controllable parameters such as the propellant species, mass flow rate, electrode geometry, AF strength, and current.[4,7] Each model includes a nondimensional free parameter with unknown dependencies. It is this free parameter that we hope to experimentally determine as accurately as possible, without any assumptions as to the nature of the gasdynamic and self-field thrust components, so that we can learn which controllable parameters it depends on. We briefly summarize the thrust models used for comparison with the data gathered on our thruster.

Fradkin et al. derive an expression for the total amount of azimuthal kinetic energy generated by the torque produced as a result of the cross product of the radial current and axial applied magnetic field within a cylindrical anode volume.[1] This energy is presented as an upper limit for the total amount of energy available for conversion into axial kinetic energy. Assuming all of the energy is converted, the corresponding thrust generated is

$$T^*_{\mathrm{AF}} = \frac{JB_{\mathrm{A}}\left(r_{\mathrm{ae}}^2 - r_{\mathrm{c}}^2\right)}{\sqrt{2\left(r_{\mathrm{ae}}^2 + r_{\mathrm{c}}^2\right)}}, \tag{2}$$

where T^*_{AF} is the maximum possible theoretical AF thrust component, J is the total current, B_{A} is the magnetic field strength, which is assumed to be uniform through the cylindrical anode volume, and r_{ae} and r_{c} are the radii of the anode and cathode respectively. Albertoni et al. relate this maximum thrust to the actual thrust by multiplying by a free parameter, χ, representing the percentage of the maximum possible thrust actually achieved. χ is found empirically on the Alta 100 kW argon AF-MPDT to be $\simeq 0.25$, where B_A was taken to be the field strength at the tip of the cathode.[7]

In order to compare between different thrusters, we use thrust data taken at the Moscow Aviation Institute (MAI) on our 30 kW LiLFA,[11–13] and subtract from the total thrust, both the self-field component,

$$T_{\mathrm{SF}} = \ln(r_{\mathrm{ae}}/r_{\mathrm{c}}) \times 10^{-7} J^2, \tag{3}$$

as well as the gasdynamic component,

$$T_{\mathrm{GD}} = \dot{m} a_0 + p_{\mathrm{c}} A_{\mathrm{c}}, \tag{4}$$

where a_0 is the ion sound speed, p_{c} is the pressure at the cathode exit, and A_{c} is the area of the cathode exit. Eqs. 3 and 4 are used for these thrust components in both Refs. 7 and 14 except for the inclusion of a small constant in the self-field component in the former source. For our 30 kW LiLFA, $r_{\mathrm{ae}} = 42$ mm and $r_{\mathrm{c}} = 12$ mm, as shown schematically in Ref. 15. We see in Figure 1a that a χ value of 0.15 agrees with the inferred T_{AF} data. However, several assumptions are made in determining both T_{SF} and T_{GD} lending uncertainty to our inferred T_{AF} values. For example, the self-field term is independent of propellant species and the derivations of both components simplify or neglect the geometry of the anode. As a result, the vertical error on the values presented in Figure 1a is undeterminable and the error on the value of χ for a particular thruster is also undeterminable.

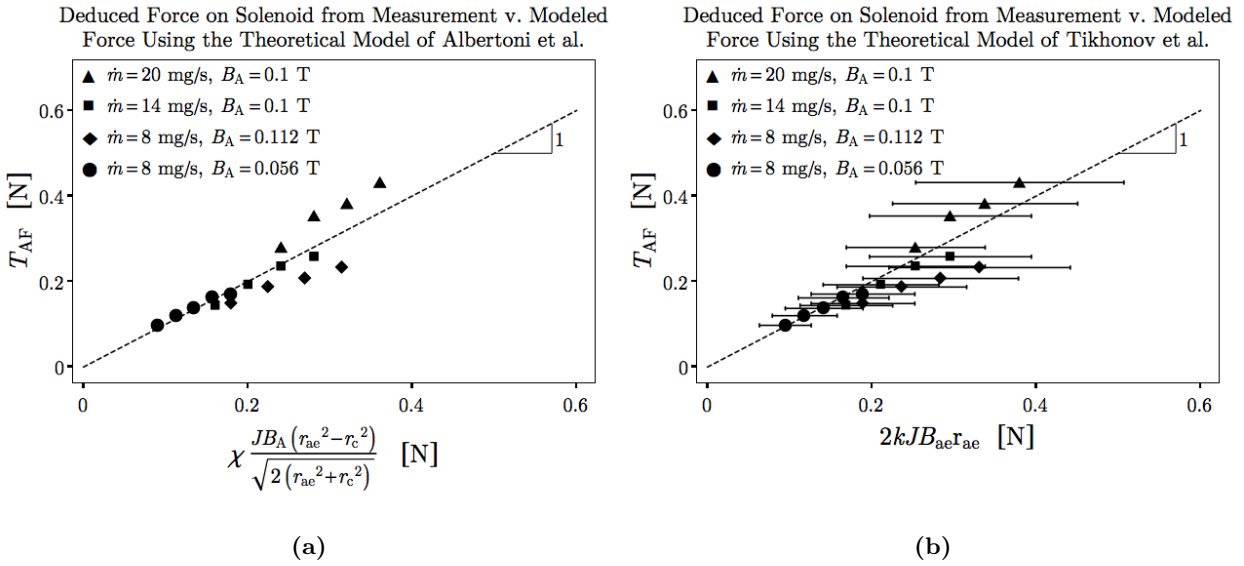

Figure 1: The y-axis of each plot represents the thrust data taken at MAI on the 30 kW LiLFA[11–13] with the theoretical gasdynamic and self-field components subtracted out. In (a), the x-axis represents the theoretical value for the AF thrust component using the derived model of Albertoni et al. with a free parameter $\chi = 0.15$. The x-axis in (b) represents the theoretical value for the AF thrust component using the model of Tikhonov et al., with k ranging from 0.1 to 0.2 as shown by the error bars.

Tikhonov et al. derive a model empirically based on measurements of density, ion velocity, electron temperature, and magnetic field profiles within the anode volume.[4] However, they come to a similar expression to that of Albertoni et al. in the limit $r_{\mathrm{ae}} \gg r_{\mathrm{c}}$ with a free parameter, k, to fit the data. They find

$$T_{\mathrm{AF}} = 2kJB_{\mathrm{ae}} r_{\mathrm{ae}}, \tag{5}$$

where B_{ae} is the magnetic field strength at the anode exit plane. This model is of particular interest to our work as the data upon which the model is based was gathered on lithium propellant AF-MPDTs, providing

a suitable comparison to our data. Additionally, our 30 kW LiLFA was designed and constructed at the MAI based on the research of Tikhonov et al.

Measurements of the total thrust taken on the 30 kW LiLFA at MAI with the theoretical self-field and gasdynamic components subtracted are presented in Figure 1b against the Tikhonov et al. model. For the 30 kW LiLFA, B_{A} is measured at the tip of the cathode and $B_{\mathrm{A}} = 3B_{\mathrm{ae}}$ along the thruster centerline. The results are nearly identical to those in Figure 1a. A least-squares minimization of each model gives $\chi = 0.152$ and $k = 0.144$, with an average difference of 32 mN between the inferred force and modeled force for both models.

While each model gives a decent qualitative fit for our thruster over a range of operating parameters, the free parameters χ and k are based on values with unknown error, and vary widely from one thruster to another as reported in the literature. For example, Alta's reported value of $\chi \simeq 0.25$ for the 100 kW argon thruster is 64% higher than the value found to best fit the 30 kW LiLFA data. In order to maximize these free parameters and the corresponding thrust generated, we must determine their dependencies on controllable parameters. We can make this determination experimentally, by means of a direct measurement of the AF thrust component.

III. Thrust Stand Design and Calibration

In order to directly measure the AF thrust component, we constructed a novel thrust stand, illustrated in Figure 2. This thrust stand is an inverted pendulum, similar to that used to measure the total thrust on the LiLFA described by Cassady et al. in Ref. 16. The difference is that the flexures support only the solenoid, which can move independently of the thruster that is fixed to the lab reference frame. The flexures are copper pipes, which carry all current and cooling necessary to operate the solenoid. Because the AF component of the thrust exerts an equal and opposite force on the solenoid, a measurement of the deflection of this inverted pendulum can be used to determine T_{AF} directly.

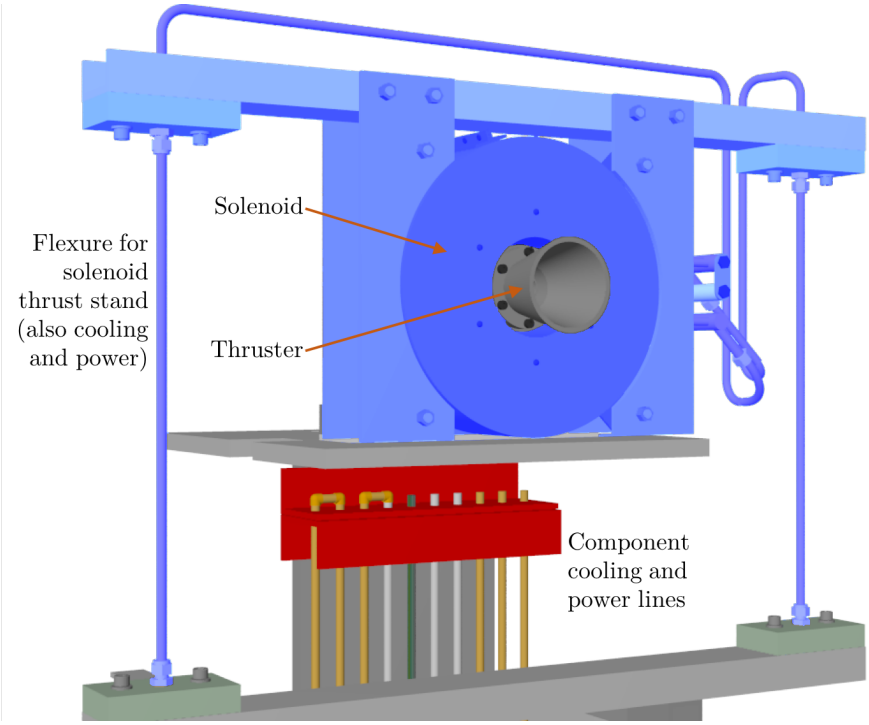

Figure 2: Schematic of the solenoid thrust stand built at the Electric Propulsion and Plasma Dynamics Laboratory for measurement of the AF component of the thrust from an AF-MPDT. The thruster is fixed in the lab frame of reference and the solenoid is supported by two flexures, allowing it to move independently of the thruster. Moving components are shown in blue. This setup is easily reconfigured between firings to take either AF component or total thrust measurements.

A. Design

The design process took into account the primary error sources found by Cassady et al., namely thermal drift and electromagnetic tare forces that contributed to a combined measurement error $> 18\%$.[16] They found that changes in the flexure temperature during calibration changed the spring constant before the calibration was complete. This effect was eliminated in the new thrust stand by modifying the cooling system to be on an open loop, rather than a closed one, with the solenoid on an independent cooling line. The closed loop resulted in temperatures continuously rising during the course of a thruster firing. With the open loop, the temperature of the coolant in the flexures is still a function of solenoid current, but the coolant output temperature reaches steady state in under two minutes. The magnetic field can be set in advance of firing and remain constant through the calibration, so the temperature of the flexures is constant while thrust data are taken. The flexures are sufficiently shielded from radiation from the electrodes such that no temperature changes were detected while the thruster fired.

Electromagnetic tare forces described by Cassady et al. were a result of magnetic fields generated by the current-carrying flexures interacting with one another. As shown in Figure 2, we positioned the flexures as far apart, and as far from the thruster current-carrying components as was practical, and did not detect any deflection resulting from forces on the flexures. However, the solenoid itself surrounds the anode and cathode, meaning any azimuthal currents in the cabling to the electrodes result in a force on the solenoid. Preliminary measurements made by shorting the thruster electrodes showed this tare force to be on the order of the anticipated measurement.

We considered two methods to remove this electromagnetic tare force from the deflection measurements. First, a measurement can be made for a given set of operating parameters and then repeated with the solenoid current running in the opposite direction. The force from the AF thrust will be the same in each instance, but the tare force will be in opposite directions. The average of the two measurements is then equal to the AF thrust component. Alternatively, the thruster electrodes can be shorted and run under the same conditions as while firing, except without propellant. This provides the tare force, which can then be subtracted from the measurement made while firing. This method requires that the short does not contribute to or subtract from the preexisting azimuthal currents, which means it must be azimuthally symmetric and within the thruster volume. Each technique was tested with the results given in Section IVB.

B. Measurement Procedure

To correlate deflection with force, we first measure the deflection of the thrust stand using a Macro Sensors PR 750-100 LVDT, which has a sensitivity of 155 mV/V/mm. The voltage from the LVDT is recorded while firing with the solenoid coolant output temperature at steady state. Then the thruster current supply is turned off, while the solenoid continues to operate, maintaining a constant temperature in the flexures and any deflection resulting from magnetic components near the thruster. A second voltage is recorded, with the difference between the two representing the distance the thrust stand was deflected. Then, a known force is applied to the pendulum. For forces under a few newtons, the change in voltage measured as a result of deflection of the thrust stand is linear with force. Therefore, application of a single known force is sufficient to calibrate a voltage measurement. However, a number of forces are checked to insure the linearity of the response.

We apply a known force by means of a sliding scale, pictured in Figure 3. The scale translates a mass back and forth through remote control. A cable is strung from the end of the scale over a pulley and attached to the back end of the thrust stand along the thruster axis. As the mass moves further outward from the pivot point, the scale applies a greater force to the thrust stand. An actuator beneath the scale allows immediate application of a known force.

IV. Experimental Results

A. Scale Calibration

The calibration scale was connected to the thrust stand and a series of LVDT voltage measurements were made at different positions along the scale. These measurements were compared to similar measurements made with known masses attached to the thrust stand, corresponding to a known force. The scale was found to provide a force of 4.1 mN/mm, with a fit function correlating each position with a force. The

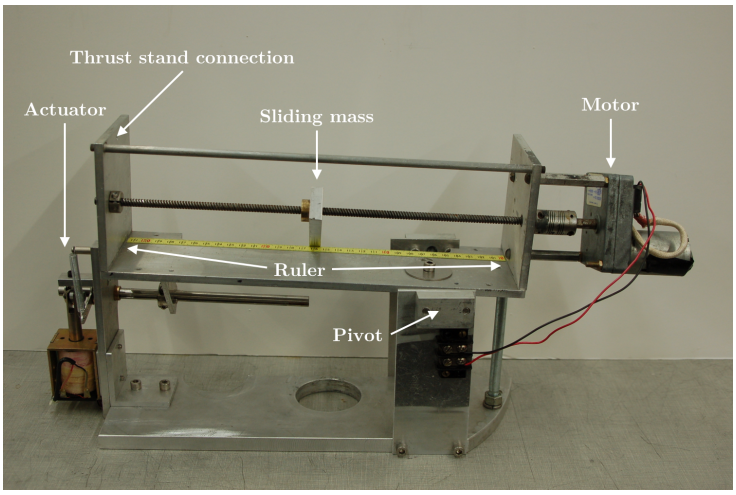

Figure 3: Calibration scale for the AF component thrust stand. The scale provides a known force by sliding a mass to a calibrated position. The known force is applied to the thrust stand by means of a solenoid actuator.

measurements from the scale are recorded to the half mm, corresponding to a resolution of $\simeq$ 2 mN from the scale. The results of this calibration are shown in Figure 4.

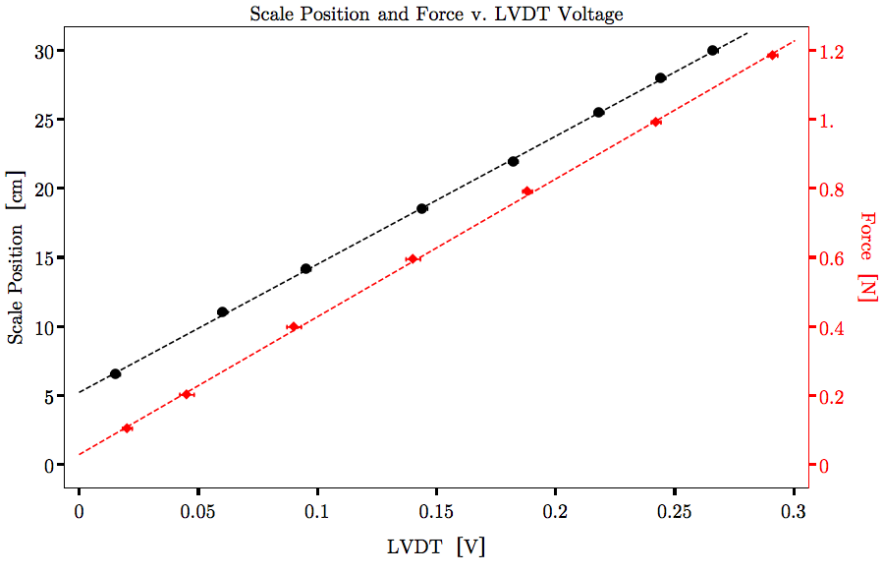

Figure 4: Calibration of the scale was performed by comparing the thrust stand deflection resulting from a given position to the deflection due to a known mass.

B. Thrust Measurements

The LiLFA was fired at 400 A, with an AF strength of 0.056 T and 8 mg/s lithium mass flow rate. Background pressure was maintained under 5×10^{-5} Torr. Once the solenoid was allowed to run for about two minutes, the coolant output temperature reached a steady value of 28.2° C and did not vary by more than 0.1° C while measurements were taken, supporting our assertion that radiative heating did not effect flexure sensitivity.

Two measurements were taken for the same operating parameters, shown in Figure 5. First, the total deflection of the stand was measured while operating with the force resulting from the interaction of the azimuthal currents to the electrodes with the applied magnetic field parallel to the force resulting from thrust

generation. The current direction was reversed through the solenoid and a second measurement was taken with the applied magnetic field antiparallel to its previous orientation.

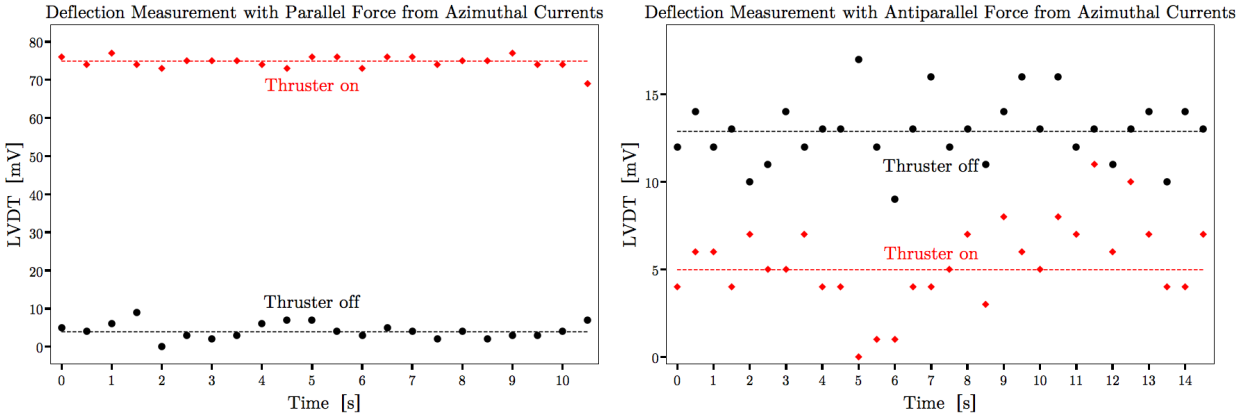

Figure 5: The deflection of the thrust stand was measured twice while firing with the same parameters. First, the thruster was fired with the force on the stand resulting from the interaction of the azimuthal currents to the electrodes with the applied magnetic field parallel to the force resulting from thrust generation, shown in (a). Next, this was repeated with these forces antiparallel, shown in (b). The average of the two measurements is the force on the solenoid resulting from thrust.

The thrust stand was calibrated with its flexures at operating temperature and found to have a sensitivity of 3.4 mN/mV. Averaging the measurements from each solenoid configuration yields a force of 108 ± 14 mN. Because the tare force is on the order of the the thrust generated, we verified this measurement with a second calibration by measuring the force generated by a shorted thruster. The region surrounding the cathode was packed with copper wire to form an azimuthally symmetric connection to the anode. We measured the tare force to be 137 ± 17 mN, which combined with the parallel force measurement yields 106 ± 19 mN and combined with the antiparallel force measurement yields 111 ± 20 mN. These results are summarized in Table 1.

Our three thrust values for the same operating conditions are in agreement. We take this as validation for the first method used, where the solenoid is run in both directions and the measurements are averaged. Shorting the thruster at higher current values, which we will pursue in subsequent tests, will result in high temperatures, making the former method advantageous.

Table 1: Results of each thrust measurement technique.

Method	Measurement	Error
Alternating B-field	108 mN	$\pm$14 mN
Parallel Tare	106 mN	$\pm$19 mN
Antiparallel Tare	111 mN	$\pm$20 mN

Our thrust error is 13% of the measurement, which is a substantial improvement over the measurements made using the previous thrust stand built for the LiLFA ($> 18\%$). Because we do not expect the operating parameters to affect the magnitude of our error, we expect the error percentage will decrease at higher power levels.

Each of our thrust measurements requires two independent deflection measurements, the errors from which result in a larger error in the final calculated thrust value. We can reduce our error by streamlining our measurement process in certain cases. A single deflection can be used to investigate any effects of mass flow rate on χ or k, as the mass flow rate can be changed while firing. There will be no change in the electromagnetic tare force for changes in $\dot{m}$. A single deflection measurement was found to have errors as small as 9 mN, compared to 14 mN for the alternating B-field method.

Our measurements are in agreement with the inferred AF thrust value shown in Figure 1, which gives 96 mN for our operating parameters. When using the least-squares optimization values for χ and k, both

presented thrust models agree with our method of subtracting the electromagnetic tare force, but underpredict by 3 mN our method of reversing the magnetic field and averaging.

V. Conclusion

We presented a proof-of-concept experiment that provides the first direct measurement of the AF component of the thrust generated by an AF-MPDT. Errors resulting from thermal drift, which limited the preexisting thrust stand for the LiLFA, have been eliminated. We found that electromagnetic tare forces can be accounted for by averaging measurements with the magnetic field running in opposite directions.

Now that this diagnostic has been validated, we can make a detailed study of the parameter space. Taking measurements with different propellants, mass flow rates, electrode geometries, magnetic field strengths, and power levels will provide an empirical relation for χ or k. This empirical relation, in turn, can be used to maximize the thrust generated and to inform a physical model for AF-MPDT thrust generation.

Acknowledgments

This research was carried out with support from the Program in Plasma Science and Technology through the Princeton Plasma Physics Laboratory. We are grateful to Bob Sorenson for all of his technical assistance in the development of our new thrust stand and calibration system, and to Dan Lev, who has lent his experience with the LiLFA on numerous occasions.

References

[1]Fradkin, D. B., Blackstock, A. W., Roehling, D. J., Stratton, T. F., Williams, M., and Liewer, K. W., "Experiments Using a 25 kW Hollow Cathode Lithium Vapor MPD Arcjet," In AIAA 7$^{\text{th}}$ Electric Propulsion Conference, Williamsburg, VA, AIAA-69-2417, 1969.

[2]Sasoh, A. and Arakawa, Y., "Thrust Formula for Applied-Field Magnetoplasmadynamic Thrusters Derived from Energy Conservation Equation," Journal of Propulsion and Power, Vol. 11, No. 2, 351-356, 1995.

[3]Tahara, H., Kagaya, Y., and Yoshikawa, T., "Performance and Acceleration Process of Quasisteady Magnetoplasmadynamic Arcjets with Applied Magnetic Fields," Journal of Propulsion and Power, Vol. 13, No. 5, 651-658, 1997.

[4]Tikhonov, V. B., Semenikhin, S. A., Alexandrov, V. A., Dyankonov, G. A., and Popov, G. A., "Research of Plasma Acceleration Processes in Self-Field and Applied Magnetic Field Thrusters," In 23$^{\text{rd}}$ International Electric Propulsion Conference, Seattle, WA, USA, IEPC-93-076, 1993.

[5]Coletti, M. "Simple Thrust Formula for an MPD Thruster with an Applied-Magnetic Field from Magnetic Stress Tensor," In 43$^{\text{rd}}$ AIAA/ASME/SAE/ASEE Joint Propulsion Conference & Exhibit, Cincinnati, OH, AIAA-2007-5284, 2007.

[6]Herdrich, G. et al., "Advanced Scaling Model for Simplified Thrust and Power Scaling of an Applied-Field Magnetoplasmadynamic Thruster," In 46$^{\text{th}}$ AIAA/ASME/SAE/ASEE Joint Propulsion Conference & Exhibit, Nashville, TN, AIAA-2010-6531, 2010.

[7]Albertoni, R., Paganucci, F., and Andrenucci, M., "A Phemenological Model for Applied-Field MPD Thrusters," Acta Astronautica. Vol. 107, 177-186, 2015.

[8]Cory, J. S., "Mass, Momentum and Energy Flow from an MPD Accelerator," PhD Thesis, Princeton University, Princeton, NJ, USA,1971.

[9]Choueiri, E. Y. and Ziemer, J. K., "Quasi-Steady Magnetoplasmadynamic Thruster Measured Performance Database," In 34$^{\text{th}}$ Joint Propulsion Conference, Cleveland, OH, 1998. AIAA-98-3472.

[10]Brown, D., Beal, B., and Haas, J., "Air Force Research Laboratory High Power Electric Propulsion Technology Development," IEEEAC, 2009.

[11]Kim, V., Tikhonov, V., and Semenikhin, S., "The First Quarterly Report on the Stage No. 3 A of the Contract on the Research Studies No. NASW-4851 between RIAME MAI and NASA," Technical Report, Moscow Aviation Institute (MAI), Moscow, Russia, April 1996.

[12]Kim, V., Tikhonov, V., and Semenikhin, S., "The Fourth Quarterly (Final) Report on the Stages No. 3 C, D of the Contract on the Research Studies No. NASW-4851 between RIAME MAI and NASA," Technical Report, Moscow Aviation Institute (MAI), Moscow, Russia, April 1997.

[13]Popov, G., Kim, V., Tikhonov, V., Semenikhin, S., and Tibrina, M., "The Fourth (Final) Quarterly Report on the Milestones (a) (4) and (a) (5) (D) of SoW of Contract No. 960938 between RIAME MAI and JPL (Items 8 and 9 of Delivery Schedule)," Technical Report, Moscow Aviation Institute (MAI), Moscow, Russia, December 1998.

[14]Tikhonov, V. B., Semenikhin, S., Brophy, J. R., and Polk, J. E., "The Experimental Performances of the 100 kW Li MPD Thruster with External Magnetic Field," In 24$^{\text{th}}$ International Electric Propulsion Conference, Moscow, Russia, IEPC-95-105, 1995.

[15]Lev, D. R. and Choueiri, E. Y., "Scaling of Efficiency with Applied Magnetic Field in Magnetoplasmadynamic Thrusters," Journal of Propulsion and Power, Vol. 28, No. 3, 609-616, 2012.

[16]Cassady, L. D., Kodys, A. D., and Choueiri, E. Y., "A Thrust Stand for High-power Steady-state Plasma Thrusters," In 38$^{\text{th}}$ Joint Propulsion Conference, Indianapolis, CA, 2002. AIAA-2002-4118.